Environmental
Research & Technology

Research Article

Investigation of land surface temperature heterogeneity in municipal landfills by satellite images

Sedat YALÇINKAYA[*1] ⓘ, **Fatih DOĞAN**[2] ⓘ

[1]*Department of Environmental Engineering, Marmara University, İstanbul, Türkiye*
[2]*Department of Urban Regeneration, İzmir Katip Çelebi University, İzmir, Türkiye*

ABSTRACT

With the increasing population and urbanization, the amount of municipal solid waste (MSW) is increasing day by day. As a result, problems such as odor, fire, and intense biogas formation originate from landfills. In order to detect and solve these problems, landfills should be monitored regularly. Geographic Information Systems (GIS) and Remote Sensing offer fast and practical solutions for the regular monitoring of landfills compared to field studies. In this study, Kömürcüoda landfill on the Anatolian side of İstanbul is monitored throughout 2022 with open source Landsat8/9 and Sentinel-2 satellite images. In this context, the surface temperature heterogeneity of the landfill was mapped by generating Land Surface Temperature (LST) images for the landfill from the Landsat thermal band. Points with statistically significant high - low LST values were determined with Hot Spot Analysis. The average annual LST for 2022 was calculated as 25.5 °C. It was observed that LST had the highest values during the summer season and the lowest values during the winter season. Additionally, it has been determined that there are persistent hot spots and cold spots in the landfill. This study presents a simple methodology using open source satellite data to monitor LST and detect LST abnormalities on landfills.

Cite this article as: Yalçınkaya S, Doğan F. Investigation of land surface temperature heterogeneity in municipal landfills by satellite images. Environ Res Tec 2023;6(4)359–370.

INTRODUCTION

Solid waste is solid materials with different contents that must be disposed of by being removed from people for social and environmental health. In Türkiye, the collection and management of municipal solid waste (MSW) is the responsibility of district municipalities. The management of MSW consists of the following steps: the generation of solid waste at its source and temporary storage at designated collection points, collection and transfer to the nearest transfer facility, transportation to the landfill, and landfilling [1–3].

The amount of waste produced is constantly increasing due to reasons such as population growth, industrialization -

urbanization, and the composition of the waste produced is changing with technological developments and differentiating consumption habits [4]. Landfills have become an important problem in recent years due to the reasons such as creating an irritating odor, negatively affecting the ecological balance around it, polluting ground and surface waters, disrupting the aesthetics of the city, creating a breeding ground for insects, rodents and microbes that may threaten human health [5]. Also, previous studies have stated that waste fires constitute an important part of fire cases [6] and fires in some landfills continue for a long time [7]. MSW in Türkiye contains a significant amount of organic waste [8]. Organic wastes in landfills are biodegraded under an-

aerobic conditions and cause biogas formation. Generally, 50–70% of biogas is Methane (CH_4) and Carbon Dioxide (CO_2), which are the main greenhouse gases [9]. Considering that 2.6% (14.7 million tons of CO_2 equivalent) of Türkiye's greenhouse gas emissions in 2021 are caused by waste management [10], landfills can be considered as important greenhouse gas sources. Consequently, the landfill monitoring emerges as a clear necessity for identifying and tracking warm biogas leakages and waste fires.

The regular landfill monitoring is possible with some in-situ measurements and field studies, but these approaches require time, cost and effort. At this point, Geographic Information Systems (GIS) – Remote Sensing based approaches are effective alternatives for regular monitoring of landfills [11]. Land Surface Temperature (LST), which can be produced from satellite or Unmanned Aerial Vehicle (UAV) data with a thermal sensor, is widely used in related studies. Faisal et al. [12] examined landfills in Kuwait and Canada, generating LST using Landsat satellite imagery from 2007–2008. They also converted LST images into contours, detecting 5 suspicious waste dumps in the densely overlapping regions of the Al-jleeb landfill in Kuwait. Additionally, a positive Methane (CH4) - LST correlation was found for the Trail Road landfill in Canada. Abu Qdais and Shatnawi developed an Artificial Neural Network (ANN) architecture to predict LST using variables such as ambient temperature, humidity, wind velocity, evaporation, emitted methane, waste amount in their study for a landfill in Jordan [13]. They also determined a significant correlation (r = 0.884) between the amount of waste stored in the landfill and the LST. Fjelsted et al. [14] used an Unmanned Aerial Vehicle (UAV) equipped with a thermal sensor to generate high-resolution LST for two landfills in Denmark. In the study, the landfill gas (LFG) - LST relationship is presented by making use of some methane (CH_4) and carbon dioxide (CO_2) measurements. Nazari et al. [15] generated LST from Landsat satellite imagery for the Bridgeton landfill in the United States, demonstrating that LST anomalies correspond to known subsurface fires within the landfill. Karimi et al. [16] examined the thermal zone distribution of 8 different landfills in Canada, highlighting that LST data could be a suitable indicator for determining landfill biothermal zones. In another study in the literature, a methodology to detect fugitive landfill gas hot spots using LST is presented for a Canadian landfill. In this context, a model that predicts high resolution LST was developed by combining Landsat 8 and Sentinel-2 satellite image bands. It was emphasized that high consistency was observed between the real LST and the predicted LST [17]. Grondona et al. [18] downscaled Landsat 8 LST with the MHUTS (Modified High-resolution Urban Thermal Sharpener) method by combining Landsat 8 and Sentinel-2 satellite data. The downscaled LST was used to detect heat islands in a Brazilian landfill. The authors confirm in the study that the downscaling method does not compromise the accuracy of LST data. Chavan et al. [19] studied a landfill in Delhi, examining waste properties, CO levels, and LST. The study revealed that older waste exhibits a higher propensity for spontaneous combustion compared to fresh waste. Mahmood et al. [20] conducted a study using LST as an indicator, presenting satellite-based bio-thermal impact insights into MSW open dumps. These literature findings underscore the availability of various satellite-based imaging and analysis methods to comprehend potential of landfills on the environment and monitor these impacts.

This study presents a detailed investigation conducted on the Kömürcüoda landfill in İstanbul. LST images obtained from Landsat 8 and Landsat 9 satellites were used to examine the seasonal and monthly variations in the study area. Additionally, Sentinel-2 satellite images were acquired to analyze the higher-resolution RGB images of the study area. The downloaded satellite images were selected to include representative samples from each month of the year 2022. Particularly in the LST images generated for the landfill area, significant high and low temperature values were identified using the hot spot analysis method. This analysis enables us to comprehend the thermal behavior of the landfill and estimate its potential environmental impacts.

MATERIALS AND METHODS

The steps followed in the study can be summarized as follows: 1) Data collection, 2) geodatabase design and generation, 3) LST calculation, 4) base map creation, and 5) hot spot analysis (Fig. 1).

Study Area
Located at the intersection of two continents (Asia and Europe), İstanbul is Türkiye's most populous city with a population of 15,907,901 [21]. 16,000 tons of MSW per day is stored in 2 landfills in İstanbul, excluding recycling and recovery processes. 10,500 tons of this waste is disposed in Silivri - Seymen Landfill on the European side, and 5,500 tons in Şile - Kömürcüoda Landfill on the Asian side [22]. In this study, the Kömürcüoda Landfill on the Asian side of İstanbul was determined as the study area (Fig. 2). The study area has a surface area of 2.11 km² and located within the borders of Şile district. It is located close to the Black Sea and surrounded by forests. Kömürcüoda Landfill has a MSW disposal area, a power generation facility utilizing the landfill gas, a leachate treatment facility, an industrial waste disposal area, a semi closed compost plant, and a biomethanization plant. The landfill has an electricity generation capacity of 39 MWh from landfill gas [23]. The city of İstanbul, where the study area is located, has a transitional climate between the Black Sea and the Mediterranean due to its geographical location. İstanbul's summers are hot and humid, and its winters are cold and rainy. In this city, the lowest temperature can drop to -11 °C at different times of the year, while the highest temperature can reach 40 °C. Rare snowfalls may occur between December and March. Since the study area is under the influence of humid air masses coming from the Black Sea, the annual average relative humidity is between 70% and 80%. Moreover, since its north faces the Black Sea, it is under the influence of northerly winds [24].
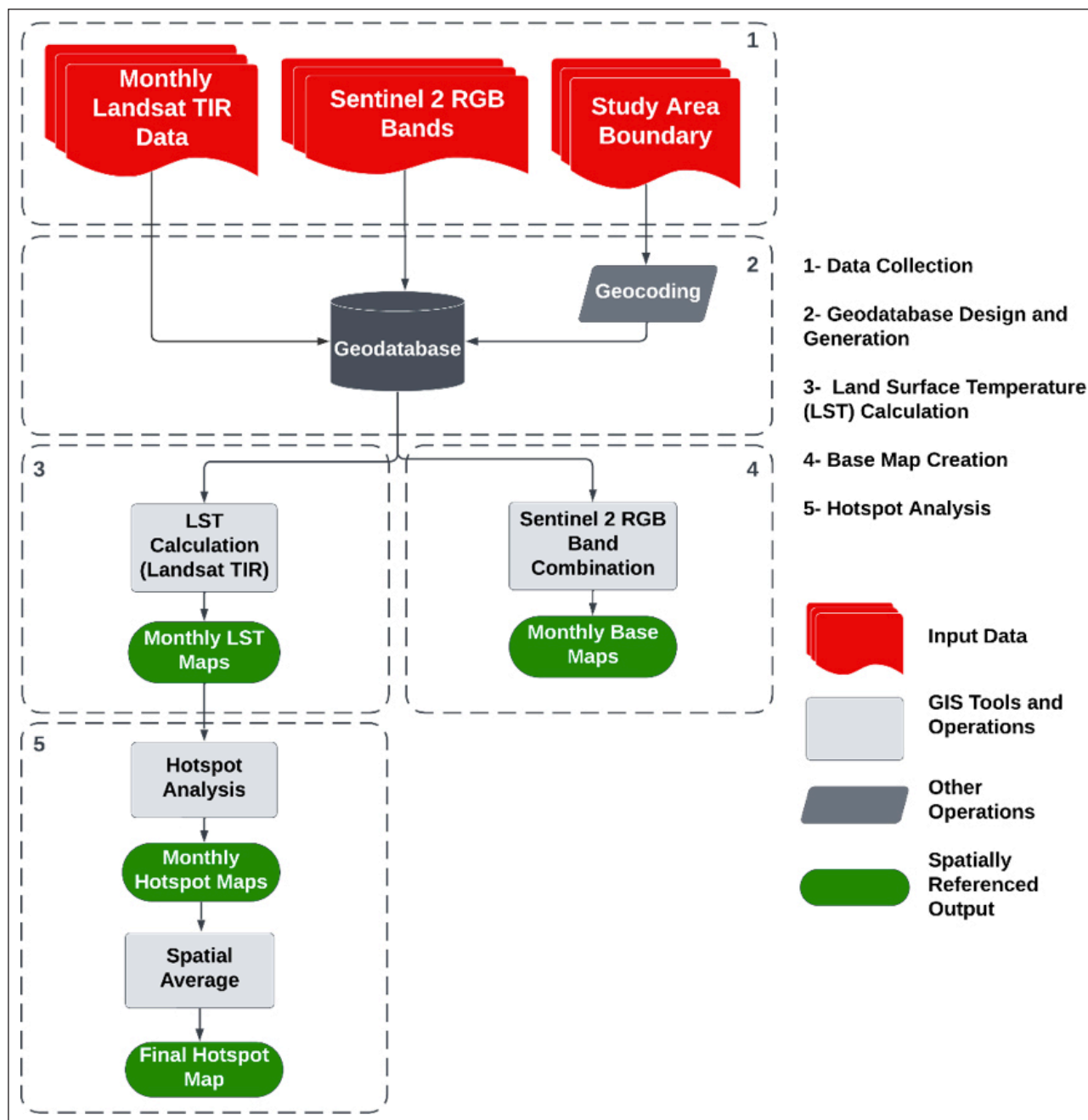
Figure 1. Stepwise methodology of the study.

Data Collection and Geodatabase Generation

The boundaries of the Kömürcüoda Landfill were manually extracted from the Google Earth Pro. The resulting KML file was transferred to the GIS environment. Landsat 8, Landsat 9 and Sentinel-2 satellite images were used in the study. An exemplary Landsat8/9 and a Sentinel-2 image were downloaded from each month of 2022. During this process, attention was paid to the temporal proximity of the Landsat and Sentinel images, to have the same path and row, and to have no cloudy images corresponding to the study area. In this context, cloud-free Sentinel and Landsat image dates were investigated for each month. If possible, Sentinel and Landsat images from the same day were downloaded. Otherwise, Landsat and Sentinel images with minimum temporal proximity among the options were paired and downloaded.

Landsat-8 and Lansat-9 satellites carry moderate resolution optical and thermal imaging systems. These systems, used to study the Earth's surface, can image the Earth's surface with a spatial resolution of up to 30 m and monitor atmospheric conditions, vegetation, oceans, glaciers, and various other land features [25]. United States Geological Survey (USGS) is responsible for managing and distributing the satellite data archive. Satellites complete their orbit around the earth approximately every 14 days and provide a new image for the same path-row coordinates every cycle. Landsat 8 and Landsat 9 contain 11 bands. First 9 bands are captured by Operational Land Imager (OLI) sensor. Bands 10 and 11 are captured by Thermal Infrared Sensor (TIRS) sensor. While 8 OLI bands have 30 m spatial resolution panchro-
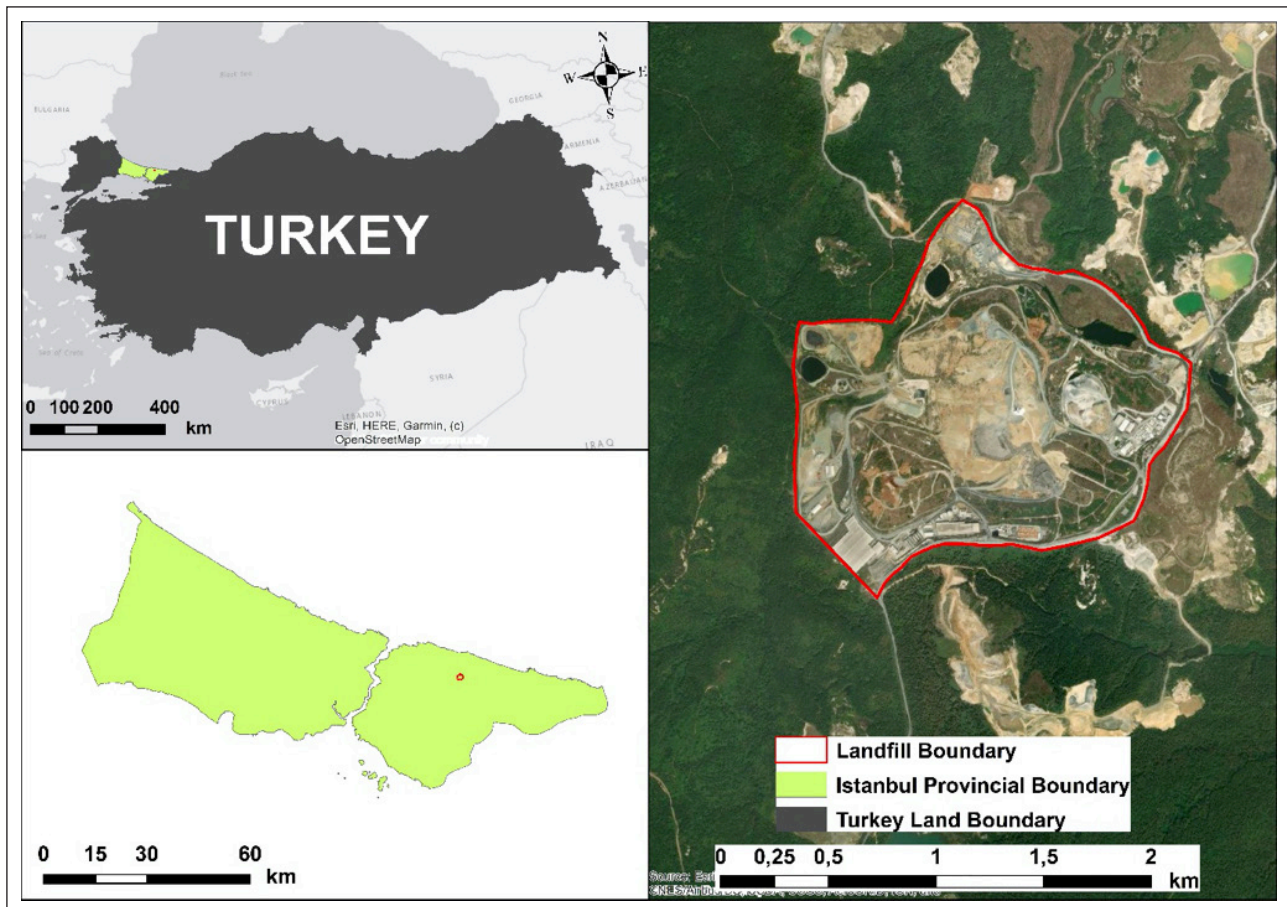
Figure 2. Study area.

matic (PAN) band has 15 m. The spatial resolution can be increased from 30 m to 15 m by pan-sharpening using the PAN band. Although TIR bands have a spatial resolution of 100 m, they are presented by resampling to 30 m. Since it is emphasized in the literature that band 11 has lower accuracy than band 10 [26], band 10 was used in LST calculations and hot spot analysis in the present study. The USGS's Earth Explorer website was used to download the Lansat-8 and Landsat-9 satellite images free of charge [27].

Sentinel-2A and Sentinel-2B are part of the Sentinel-2 satellites developed and operated by the European Space Agency (ESA). With the advanced remote sensing tools in the satellites, it can image the Earth's surface in a high resolution and multi-spectral manner. The images of these satellites can display the Earth's surface with a spatial resolution of up to 10 m. They were used in the base map creation step of the project, as they provide higher resolution and quality images compare to the Landsat images. Sentinel-2 satellites also have higher time resolution compared to Landsat satellites. They pass through an area on average every 10 days and produce an image. Sentinel satellite images were freely downloaded from the Copernicus Open Access Hub website [28]. Within the scope of the study, Landsat Collection 2 Level 2 and Sentinel Level 2A images were used, since Level 2 data products are preprocessed and do not require correction of atmospheric effects, geometric and radiometric calibrations. The satellite data list used in the study is presented in Table 1. All of the

data were converted to the WGS 1984 UTM (Universal Traverse Mercator) Zone 35 N, which is the most suitable projected coordinate system for the study area and transferred to the GIS environment. Satellite image processing and spatial analyses were performed in Esri's ArcMap software.

Land Surface Temperature (LST) Calculation
"Additive Offset" and "Multiplicative Scale Factor" values given for Band-10 in Table 6.1 in the "USGS's Landsat 8–9 Collection 2 (C2) Level 2 Science Product (L2SP) Guide" [29], an equation to convert the reflectance values given in the raw data to LST in Kelvin (K°) degrees, were used. The equation was modified to output LST in Celsius (C°) degrees:

Surface Temperature (C^o) = 0,00341802 * Reflectance Value + 149,0 −273,15   Equation 1.

Raster calculation was performed to the satellite images using the Eq. 1. The reflectance values in every 30 m by 30 m of pixels were converted to LSTs (Fig. 3). Then, the area within the study area boundaries was extracted. This process was performed to the image of each month.

Hot Spot Analysis
After LST calculations, Hot spot Analysis was performed using previously created LST maps. For this reason, ArcMap's, "Hot Spot Analysis Getis Ord Gi*" Spatial Analysis Tool was

Table 1. Identifiers of the satellite data

Landsat 8/9 Data

LC09_L2SP_180031_20220120_20230430_02_T1

LC09_L2SP_180031_20220205_20230429_02_T1

LC09_L2SP_180031_20220325_20230424_02_T1

LC08_L2SP_180031_20220402_20220411_02_T1

LC09_L2SP_180031_20220512_20230417_02_T1

LC08_L2SP_180031_20220605_20220610_02_T1

LC08_L2SP_180031_20220723_20220802_02_T1

LC09_L2SP_180031_20220816_20230402_02_T1

LC08_L2SP_180031_20220909_20220914_02_T1

LC09_L2SP_180031_20221003_20230327_02_T1

LC09_L2SP_180031_20221104_20230323_02_T1

LC08_L2SP_180031_20221230_20230110_02_T1

Sentinel 2 Data

S2A_MSIL2A_20220117T090321_N0301_R007_T35TPF_20220117T120927

S2B_MSIL2A_20220211T090009_N0400_R007_T35TPF_20220211T111741

S2A_MSIL2A_20220325T084611_N0400_R107_T35TPF_20220325T120651

S2B_MSIL2A_20220402T085549_N0400_R007_T35TPF_20220402T123301

S2A_MSIL2A_20220514T084601_N0400_R107_T35TPF_20220514T133711

S2B_MSIL2A_20220601T085559_N0400_R007_T35TPF_20220601T120802

S2A_MSIL2A_20220723T084611_N0400_R107_T35TPF_20220723T131856

S2B_MSIL2A_20220817T084559_N0400_R107_T35TPF_20220817T102926

S2B_MSIL2A_20220909T085559_N0400_R007_T35TPF_20220909T103032

S2A_MSIL2A_20221001T084801_N0400_R107_T35TPF_20221001T132601

S2B_MSIL2A_20221105T085039_N0400_R107_T35TPF_20221105T114546

S2A_MSIL2A_20221230T085351_N0509_R107_T35TPF_20221230T131052

used. To use this tool, input data must be in point format. Therefore, before applying hot spot analysis to LST rasters were converted to point format. Then, the hot spot analysis was applied to the LST maps in point format (Fig. 4).

In Hot Spot Analysis, the Getis-Ord Gi* statistic is calculated for each component. Statistically significant high-low value clusters are determined with the obtained p-values and z-scores [30]. P-value represents the probability. During Hot Spot Analysis, p-value is used to determine whether the spatial distribution of events in a region is random. If the p value is statistically significantly lower, then the events in this region are unlikely to be random. Z-score is a statistical term that shows how far a data is from the mean value in standard deviation units [31]. Getis-Ord Gi* statistic can be formulated as:

$$G_i^* = \frac{\Sigma_{j=1}^n w_i x_j - \bar{x}\Sigma_{j=1}^n w_{i,j}}{S\sqrt{\frac{[\Sigma_{j=1}^n w_{i,j}^2 - (\Sigma_{j=1}^n w_{i,j})^2]}{n-1}}}$$

Equation 2.

Where; G_i^*= statistic z-score, x_j= attribute value for feature j, $w_{i,j}$= spatial weight between feature i and j, n=total number of features, $\bar{X}$=mean, S=standard deviation

$$\bar{X} = \frac{\Sigma_{j=1}^n x_j}{n}$$

Equation 3.

$$S = \sqrt{\frac{\Sigma_{j=1}^n x_j^2}{n} - (\bar{x})^2}$$

Equation 4.

In equation 2, weighted z-score calculations are made according to the distance between the points in vector format. In order to show them more meaningfully after z-score calculation, ArcMap's Getis-Ord Gi* tool separates z-score values according to specific z-score classification. This classification was calculated according to the determined confidence levels (90%, 95%, 99%). The principle of employing a fixed distance spatial relationship revolves around the evaluation of individual features in relation to their neighboring counterparts to identify spatial clusters of high or low LST. A feature with a high value may be intriguing, but it might not necessarily constitute a statistically significant hot spot. To qualify as a statistically significant hot spot, a feature must not only possess a high value but also be situated amidst other features that also exhibit high values. The local sum of a feature and its neighboring features is assessed in relation to the total sum of all features. When this local sum significantly deviates from the anticipated local sum, and this deviation
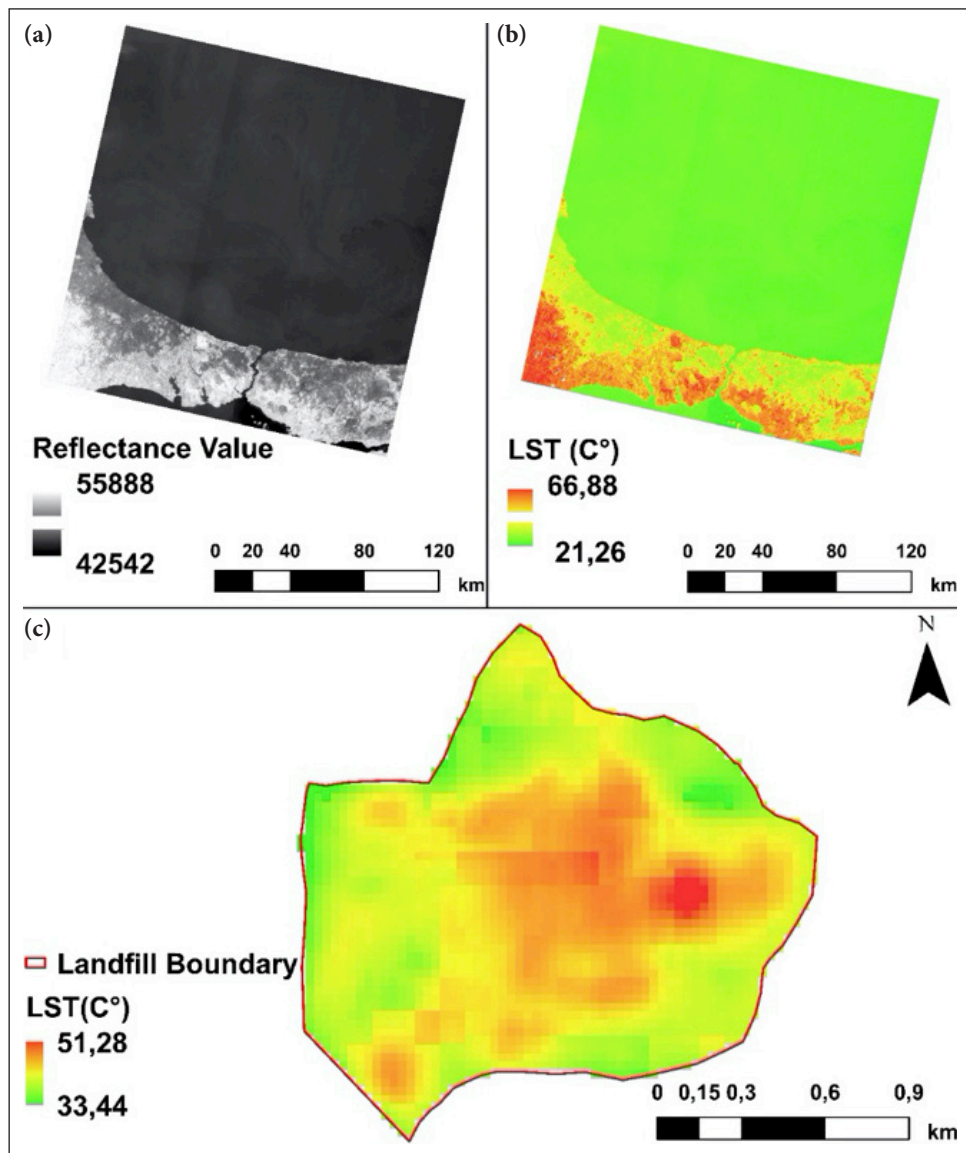
Figure 3. **(a)** Landsat thermal band, **(b)** calculated LST and **(c)** extracted landfill LST.
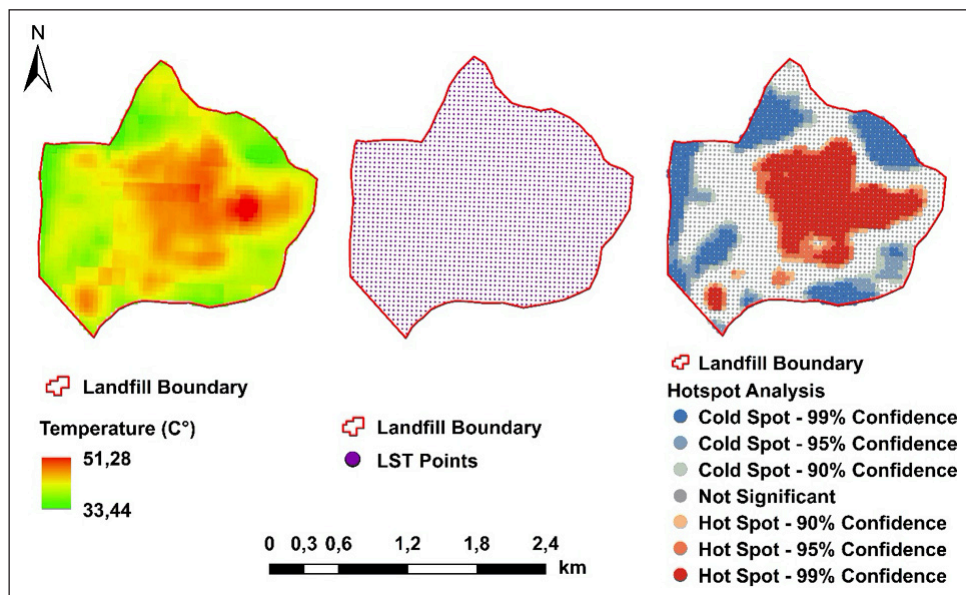

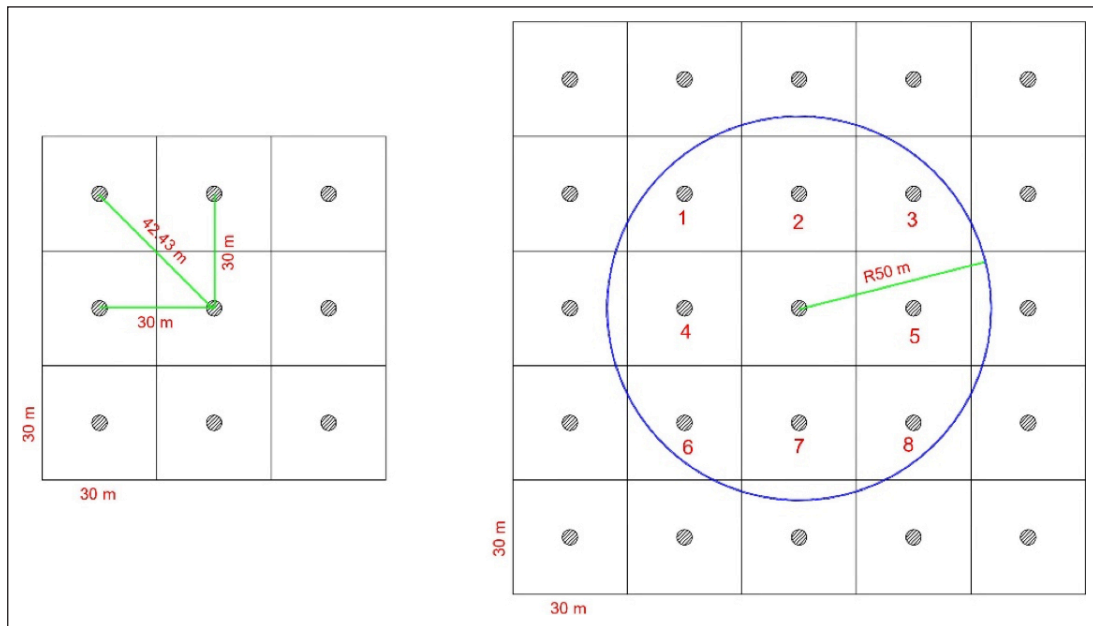**Figure 4**. LST to hot spot analysis.

Figure 5. Schematic representation of the hot spot analysis application according to the threshold distance.
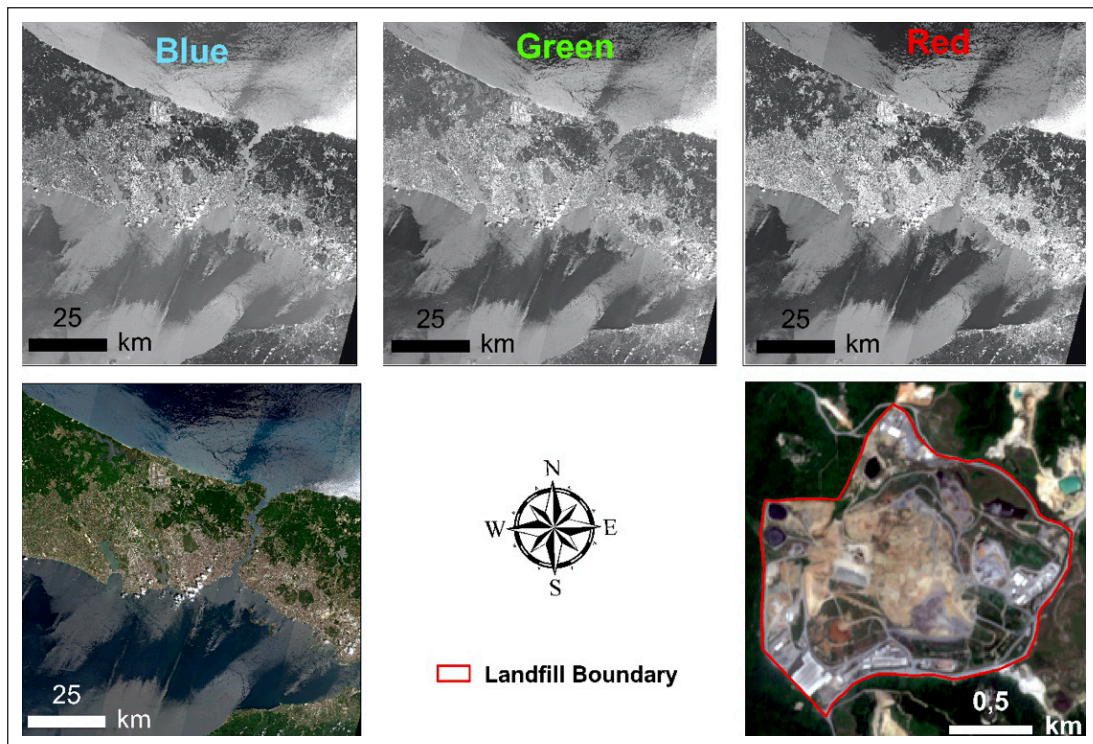

Figure 6. Base map creation process.

is too substantial to attribute to random chance, it yields a statistically significant z-score. Features situated within the designated threshold distance will carry a designated weight, consequently affecting computations pertaining to the target feature. On the other hand, neighboring features outside the threshold distance will receive a weight of zero and have no impact on computations related to the target feature. While performing the hot spot analysis, the spatial relationship was determined as fixed distance and the threshold value was entered as 50 m. Since the distance between the points obtained

from the LSTs is 30 m, each target feature was analyzed with its 8 neighboring points (Fig. 5). 50 m threshold was used to include the surrounding eight neighbors. All hot spot analyses results were integrated into a single map, in terms of the z-values, to visualize the general trend in LST abnormalities.

Base Map Creation

To better understand what is happening in the hot spots and cold spots and what could cause the temperature difference there, base maps were created for each month from
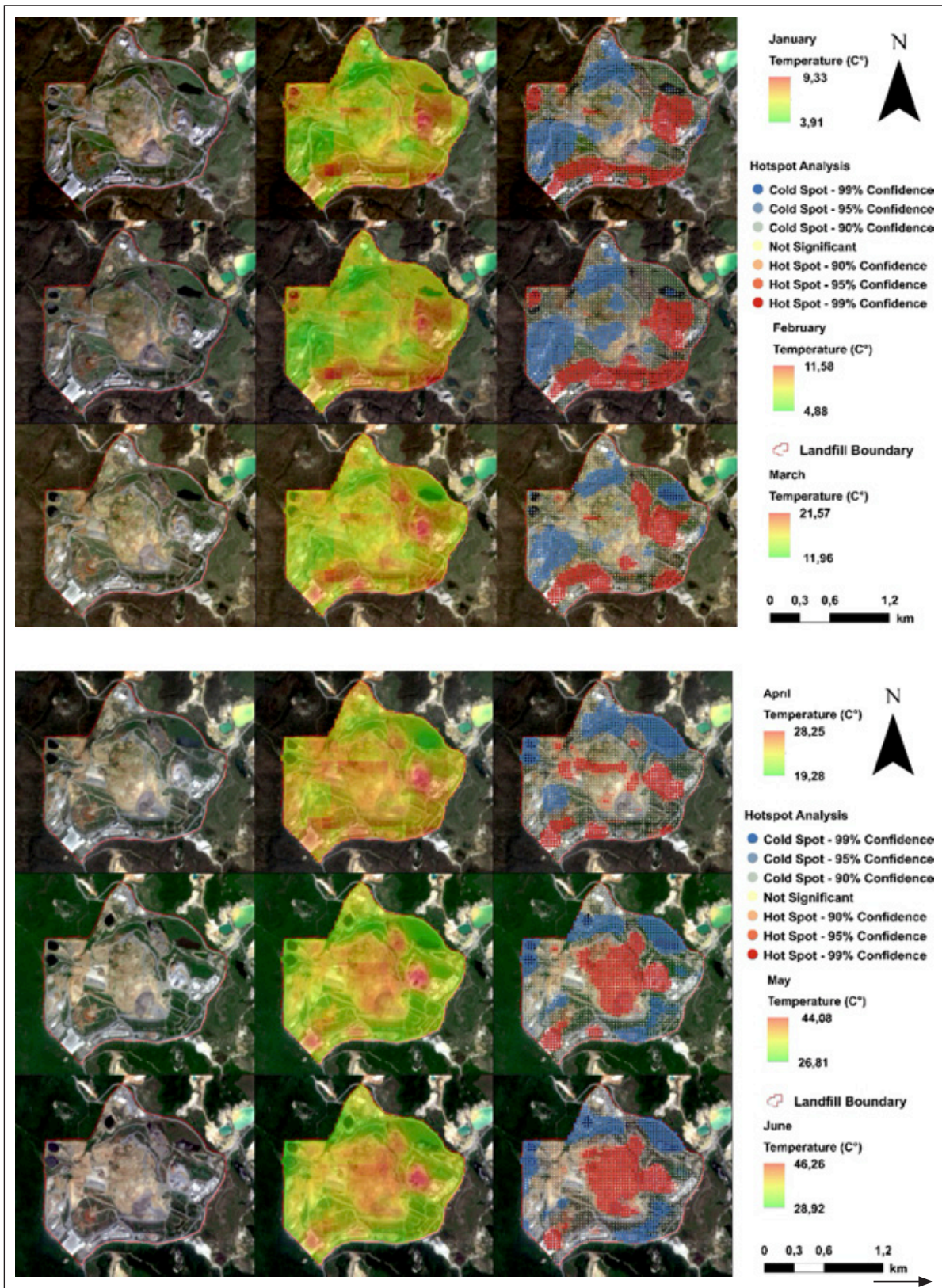
the Sentinel-2 satellite data of the closest or the same date to the Landsat satellite data which are used in LST calculation and Hot spot Analysis. For this purpose, Band 2 (blue), Band 3 (green), and Band 4 (red) from Sentinel-2 data were used as raw data. These 3 bands were combined and RGB images were produced. Area within the boundaries of the Kömürcüoda Landfill was extracted (Fig. 6). Sentinel's RGB band images (Band 2, Band 3, Band 4) were used to create the base map instead of Landsat's RGB band images, since Sentinel-2 has a higher resolution. Landsat provides 30 m x 30 m resolution images, while Sentinel has 10 m x10 m resolution images.
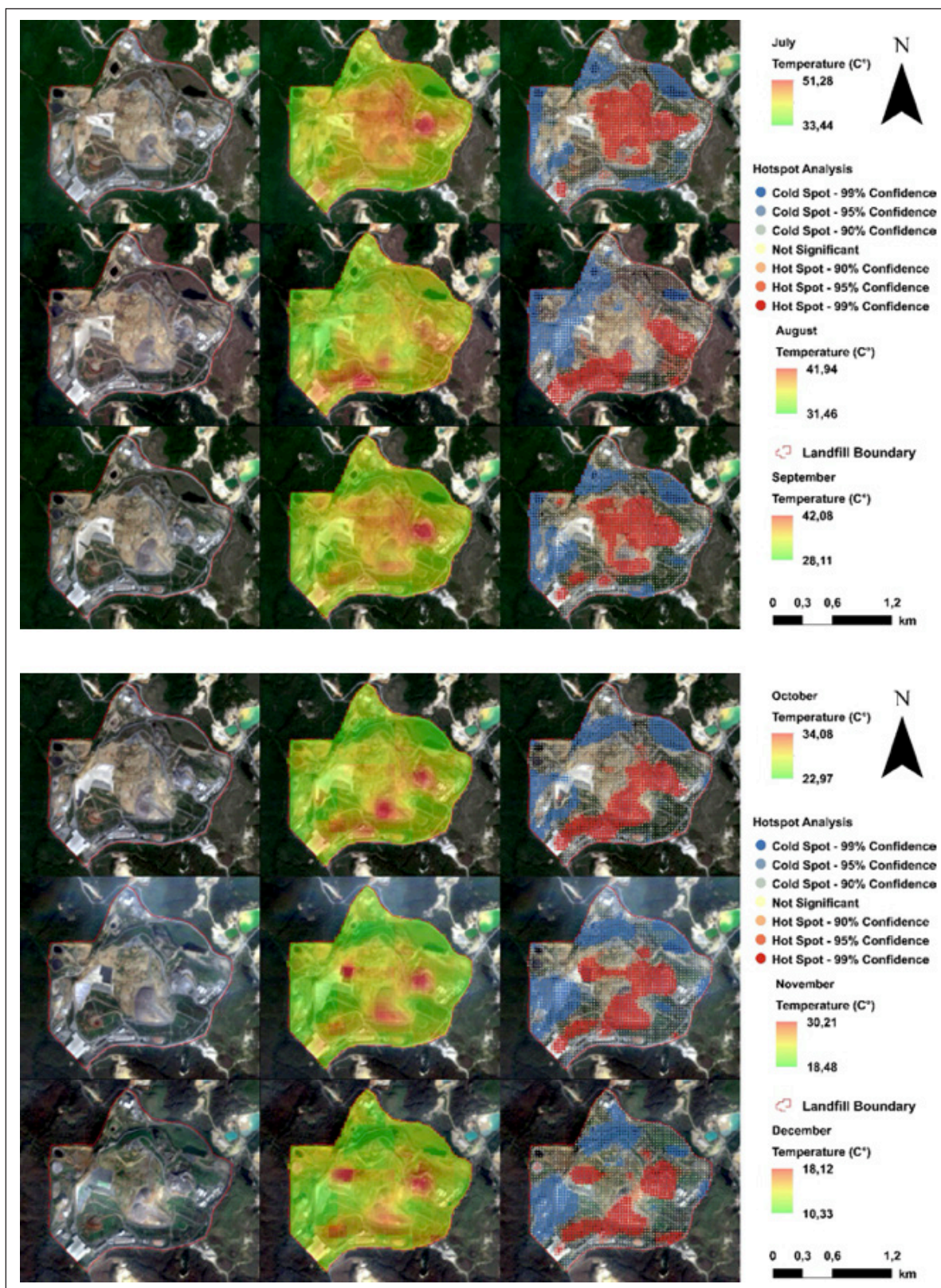
Figure 7. Base maps, land surface temperature maps and hot spot analysis result maps for 12 months of 2022.

RESULTS AND DISCUSSION

Within the scope of the study, base maps, LST and hot spot maps were produced for each month of 2022 (Fig. 7). Thus, the effect of seasonal conditions on LST was also considered. In LST rasters, low values are represented by green and high values by red. The month with the highest LST values was July, while the month with the lowest LST values was January. Significant difference between the minimum and maximum values were calculated for each
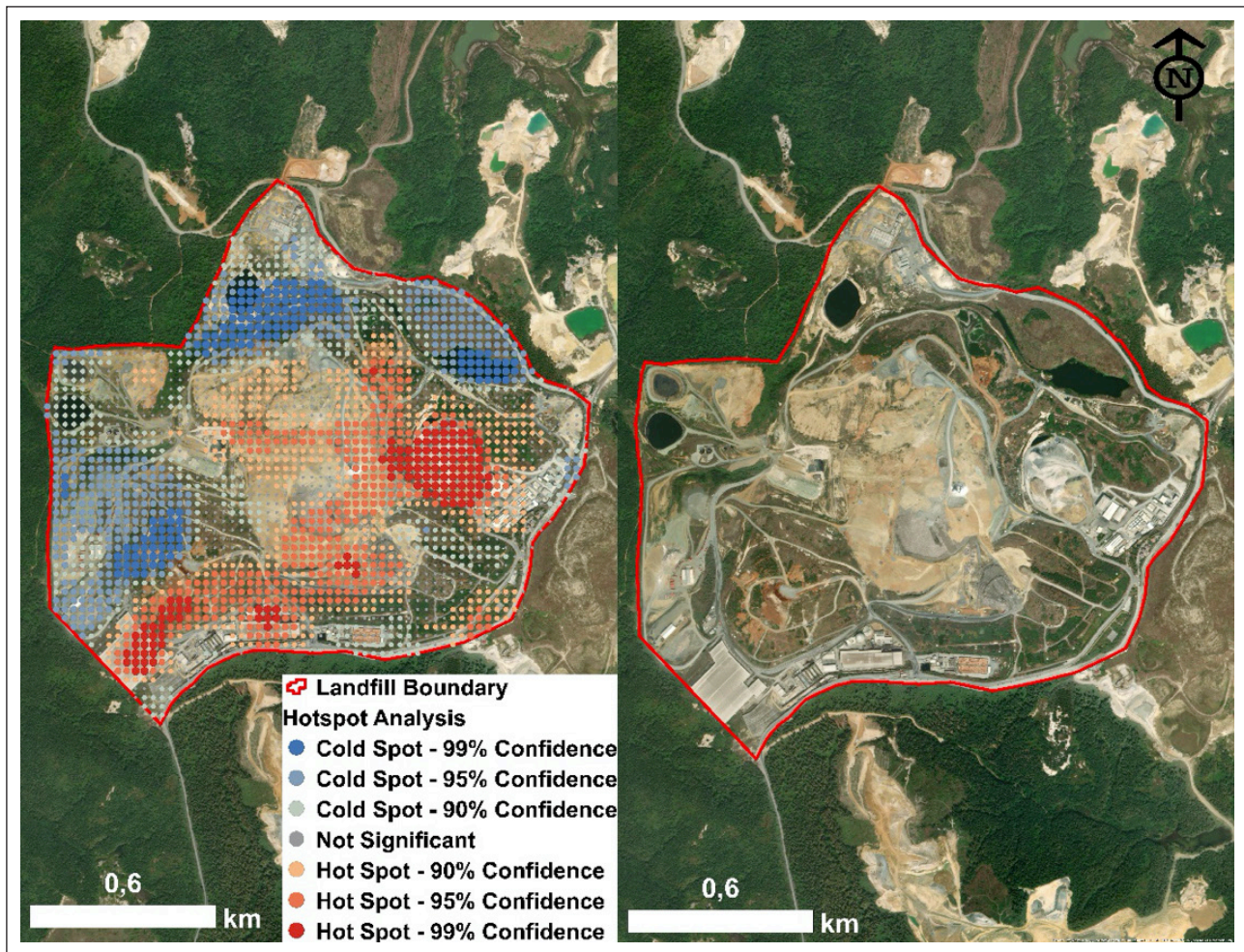
Figure 8. 12-month average hot spot analysis result map and base map.

month. The average temperature of the landfill in 2022 is calculated as 25.5 °C. Abu Qdais and Shatnawi calculated the average temperature of Al Akeedr landfill (Jordan) in 2016 as 32.4 °C [13]. This average temperature difference may be due to reasons such as the fact that the two landfills are located in regions with different climates, have different storage capacities, and are of different sizes. In addition, it has been observed that the seasonal and monthly changes of the Kömürcüoda landfill show a complex pattern. In winter, lower temperature values were observed due to the decrease in temperature and cold weather events. On the other hand, an increase in temperature was evident in the summer months, indicating an increase in thermal activity in the landfill. These findings clearly show the effect of seasonal changes on the thermal behavior of the landfill.

In the hot spot analysis results, the yellow dots are not statistically significant in terms of LST values in landfill. Red dots represent statistically significant high LST values, while blue dots represent statistically significant low LST values. These blue and red dots were classified in different confidence intervals according to the p-value and z-score values obtained as a result of the analysis. We are more interested in the LST abnormalities at high temperatures which may indicate biogas leakage.

High LST values and hot spots often determined in active landfill areas and specific areas where compost plant and co-generation plant. It has been observed that areas with vegetation on the edges of the landfill and leachate collection ponds are cold spot areas. This confirms the inverse relationship between LST and water - vegetation. The relationship of LST anomalies may be due to biogas leakage and/or underground bioconversion of organic fraction of municipal solid waste. Field studies are necessary to reach a certain conclusion.

12-month average hot spot results are presented in Figure 8. This is the holistic result of one year of LST observations for simple visualization. The presence of hot spots and cold spots spread over large areas shows that there are statistically significant high-low values that persist over one year. Nazari et al. [15] examined the Bridgeton landfill over a 17-year period and visualized locations based on the frequency of maximum or near-maximum LST values. In the current study, an approach based on spatial and statistical analysis is presented. This process provides a straightforward approach in identifying the continuous regions, as it is based on calculating the average of hot spot analysis results conducted for all months. Furthermore, applications such as trend analysis and emerging hot spot analysis can offer more detailed outcomes in determining the spatiotemporal patterns of the dataset [32].

The methodology developed in this study can be applied to any landfill for monitoring LST and detecting LST abnormalities. The study comes with certain limitations. For instance, the thermal band of the Landsat satellite with moderate resolution was utilized. It is likely that conducting a study that combines fieldwork with data from different satellites or sensors with higher sensitivity would yield more valuable results. Furthermore, only sample data from the year 2022 were used to assess the thermal behaviors of the landfill site. An investigation spanning a longer timeframe with data collected at more frequent intervals could provide a more comprehensive and reliable understanding of the thermal characteristics of the landfill. One of the most important limitations of the current study was that the satellite images contained cloudiness for many dates. In future studies on LST, the estimation of missing pixels due to cloudiness with modern approaches will be able to eliminate the problems regarding data frequency [33]. Lastly, the study examines the thermal behaviors of the Kömürcüoda landfill. Since the study area only encompasses the boundaries of the landfill, the thermal influence of the landfill to the surrounding area was not considered in this study.

CONCLUSION

The present study, which effectively utilizes open source multi temporal satellite data such as Landsat 8/9 and Sentinel-2, introduces a practical and sustainable approach for the regular monitoring of LST and LST abnormalities on landfills. Consequently, it is believed that the outcomes of this study and the applied methodology could serve as guidance for waste management authorities.

The study results reveal that LST does not exhibit a uniform structure at any given time. The relationship between LST anomalies and hot spots in the study area with phenomena like biogas leakage, sub-surface waste fires, and stored waste volume should be investigated through fieldwork and in-situ measurements. Moreover, the study area is adjacent to a forest, which prompts the examination of the thermal impact of landfill LST on the forest area in future research.

The continuous monitoring of landfills offers the potential to contribute to the resolution of issues stemming from landfill-related biogas emissions, fires, and odors. However, in order to comprehensively understand the thermal behaviors of landfills over an extended time frame, it is imperative to move beyond studies constrained by limited time periods and invest in automated, accurate, and continuously updated systems.

Averaging z-value may lose its significance for a general trend over the year. Averaging the LST value for each of the point and then performed Getis Ord Gi* analysis may be tried in the future studies. In addition, longer time periods may be studied to determine long time hot spots and evaluate inter-annual relationships.

In summary, this study's outcomes provide insights into the complexities of landfill thermal behaviors and emphasize the necessity of sustained monitoring practices, advanced technologies, and waste management strategies that align with sustainable principles.

DATA AVAILABILITY STATEMENT

The authors confirm that the data that supports the findings of this study are available within the article. Raw data that support the finding of this study are available from the corresponding author, upon reasonable request.

CONFLICT OF INTEREST

The authors declared no potential conflicts of interest with respect to the research, authorship, and/or publication of this article.

ETHICS

There are no ethical issues with the publication of this manuscript.

REFERENCES

[1] M. C. Höke, and S. Yalcinkaya, "Municipal solid waste transfer station planning through vehicle routing problem-based scenario analysis," Waste Management & Research, Vol. 39(1), pp. 185–196, 2021. [CrossRef]

[2] S. Yalcinkaya, "A spatial modeling approach for siting, sizing and economic assessment of centralized biogas plants in organic waste management," Journal of Cleaner Production, Vol. 255, Article 120040, 2020. [CrossRef]

[3] S. Yalcinkaya, and O. S. Kirtiloglu, "Application of a geographic information system-based fuzzy analytic hierarchy process model to locate potential municipal solid waste incineration plant sites: A case study of Izmir Metropolitan Municipality," Waste Management & Research, Vol. 39(1), pp. 174–184, 2021. [CrossRef]

[4] T. Bayram, Y. A. Arhun, and S. Tirink, "An Evaluation of Solid Waste Management in Turkey," Black Sea Journal of Engineering and Science, Vol. 2(3), pp. 88–91, 2019. [CrossRef]

[5] A. Sağlık, Y. S. Domaç, Ş. N. Reyhan, F. Avcı, F. Kartal, and D. Şenkuş, "Improvement and analysis of solid waste landfills example of Çanakkale Onsekiz Mart University," Academia Journal of Nature and Human Sciences, Vol 7(1), pp. 105–125, 2021.

[6] S. Yalçınkaya, F. Doğan, and H. İ. Kaleli, "Investigation of waste fires and spatial accessibility of fire stations in Izmir, Turkey," Urban Academy, Vol. 15(2), pp. 727–741, 2022. [CrossRef]

[7] J. Kret, L. Dalidowitz Dame, N. Tutlam, R. W. De-Clue, S. Schmidt, K. Donaldson, R. Lewis, S. E. Rigdon, S. Davis, A. Zelicoff, C. King, Y. Wang, S. Patrick, and F. Khan, "A respiratory health survey of a subsurface smoldering landfill," Environmental Research, Vol. 166, pp. 427–436, 2018. [CrossRef]

[8] H. Şenol, E. A. Elibol, Ü. Açıkel, and M. Şenol, "Primary Biomass Sources for Biogas Production in Turkey," BEU Journal of Science, Vol. 6(2), pp. 81–92, 2017. [CrossRef]

[9]   Y. Korkmaz, S. Aykanat, and A. Çil, "Biogas and energy production from organic wastes," SAÜ Fen Edebiyat Dergisi, SAU Journal of Science and Letters, Vol. 12, pp. 489–497, 2012.

[10]   Turkish Statistical Institute, "Sera Gazı Emisyon İstatistikleri, 1990-2021," 2023. https://data.tuik.gov.tr/Bulten/Index?p=Sera-Gazi-Emisyon-Istatistikleri-1990-2021-49672 Accessed on Jul 16, 2023.

[11]   L. G. Papale, G. Guerrisi, D. De Santis, G. Schiavon, and F. Del Frate, "Satellite data potentialities in solid waste landfill monitoring: Review and case studies," Sensors, Vol. 23(8), Article 3917, 2023. [CrossRef]

[12]   K. Faisal, M. AlAhmad, and A. Shaker, "Remote sensing techniques as a tool for environmental monitoring," The International Archives of the Photogrammetry, Remote Sensing and Spatial Information Sciences, Vol. XXXIX-B8, pp. 513–518, 2012. [CrossRef]

[13]   H. Abu Qdais, and N. Shatnawi, "Assessing and predicting landfill surface temperature using remote sensing and an artificial neural network," International Journal of Remote Sensing, Vol. 40(24), pp. 9556–9571, 2019. [CrossRef]

[14]   L. Fjelsted, A. G. Christensen, J. E. Larsen, P. Kjeldsen, and C. Scheutz, "Assessment of a landfill methane emission screening method using an unmanned aerial vehicle mounted thermal infrared camera – A field study," Waste Management, Vol. 87, pp. 893–904, 2019. [CrossRef]

[15]   R. Nazari, H. Alfergani, F. Haas, M. E. Karimi, M. G. Rabbani Fahad, S. Sabrin, J. Everett, N. Bouaynaya, and R. W. Peters, "Application of satellite remote sensing in monitoring elevated internal temperatures of landfills," Applied Sciences, Vol. 10(19), Article 6801,2020.

[16]   N. Karimi, K. T. W. Ng, A. Richter, J. Williams, and H. Ibrahim, "Thermal heterogeneity in the proximity of municipal solid waste landfills on forest and agricultural lands," Journal of Environmental Management, Vol. 287, Article 112320, 2021.

[17]   N. Karimi, K. T. W. Ng, and A. Richter, "Prediction of fugitive landfill gas hotspots using a random forest algorithm and Sentinel-2 data," Sustainable Cities & Society, Vol. 73, Article 103097, 2021.

[18]   A. Grondona, L. P. Gomes, L. M. Schiavo, M. Caetano, and B. J. B. L. Barbosa, "Use of the downscalling method in satellite images for the analysis of heat islands in landfills," Remote Sensing Applications Society and Environment, Vol. 26, Article 100702, 2022.

[19]   D. Chavan, G. S. Manjunatha, D. Singh, L. Periyaswami, S. Kumar, and R. Kumar, "Estimation of spontaneous waste ignition time for prevention and control of landfill fire," Waste Management, Vol. 139, pp.

258–268, 2022.

[20]   K. Mahmood, F. Faizi, and F. Mushtaq, "Satellite based bio-thermal impact insights into MSW open dumps: a pair-unified proximity scenario," Geomatics, Natural Hazards & Risk, Vol. 13(1), pp. 667–685, 2022.

[21]   Turkish Statistical Institute, "Adrese Dayalı Nüfus Kayıt Sistemi Sonuçları, 2022," 2023. https://data.tuik.gov.tr/Bulten/Index?p=Adrese-Dayali-Nufus-Kayit-Sistemi-Sonuclari-2022-49685 Accessed on Jul 22, 2023.

[22]   Istanbul Metropolitan Municipality, "Düzenli Depolama," 2023. http://istac.ssplab.com/tr/temiz-istanbul/evsel-atiklar/duzenli-depolama Accessed on Jul 22, 2023.

[23]   Istanbul Metropolitan Municipality, "Faaliyet Haritası," 2023.

[24]   Istanbul Governorship, "İklim." http://www.istanbul.gov.tr/iklim-istanbul Accessed Sep 22, 2023.

[25]   USGS, "Landsat Satellite Missions," 2023. https://www.usgs.gov/landsat-missions/landsat-satellite-missions Accessed on Jul 19, 2023.

[26]   J. Guo, H. Ren, Y. Zheng, S. Lu, and J. Dong, "Evaluation of land surface temperature retrieval from landsat 8/TIRS images before and after stray light correction using the SURFRAD dataset," Remote Sensing, Vol. 12(6), Article 1023, 2020.

[27]   USGS, "EarthExplorer," 2023. https://earthexplorer.usgs.gov/ Accessed on Jul 19, 2023.

[28]   ESA, "Open Access Hub," 2023. https://scihub.copernicus.eu/ Accessed on Jul 21, 2023.

[29]   USGS, "Landsat 8-9 Collection 2 Level 2 Science Product Guide," 2023. https://www.usgs.gov/media/files/landsat-8-9-collection-2-level-2-science-product-guide Accessed on Jul 24, 2023.

[30]   ESRI, "How Hot Spot Analysis (Getis-Ord Gi*) works," 2023. https://pro.arcgis.com/en/pro-app/latest/tool-reference/spatial-statistics/h-how-hot-spot-analysis-getis-ord-gi-spatial-stati.htm Accessed on Jul 26, 2023.

[31]   ESRI, "What is a z-score? What is a p-value?" https://pro.arcgis.com/en/pro-app/latest/tool-reference/spatial-statistics/what-is-a-z-score-what-is-a-p-value.htm Accessed on Sep 23, 2023.

[32]   S. Yalcinkaya, and Y. Ruhbas, "Spatiotemporal analysis framework for identifying emerging hot spots and energy potential from livestock manure in Turkey," Renewable Energy, Vol. 193, pp. 278–287, 2022.

[33]   S. Kartal, and A. Sekertekin, "Prediction of MODIS land surface temperature using new hybrid models based on spatial interpolation techniques and deep learning models," Environmental Science and Pollution Research, Vol. 29(44), pp. 67115–67134, 2022.